

## Article

# Ultrafast Hydrogen Production via Hydrolysis of MgH<sub>2</sub>-NaH Composite

Zhao Zhang <sup>1,2,3</sup>, Zhenji Li <sup>3,4</sup>, Wei Zhao <sup>3</sup>, Yushan Zhang <sup>3</sup>, Chong Peng <sup>5</sup>, Changcheng Liu <sup>3,4,\*</sup> and Li Guo <sup>3,\*</sup>

<sup>1</sup> School of Energy and Power Engineering, North University of China, Taiyuan 030051, China; zhangz\_123@163.com

<sup>2</sup> State Key Laboratory of Coal and CBM Co-Mining, Taiyuan 030051, China

<sup>3</sup> Shanxi Key Laboratory of Efficient Hydrogen Storage & Production Technology and Application, School of Materials Science and Engineering, North University of China, Taiyuan 030051, China; 13610652058@163.com (W.Z.)

<sup>4</sup> School of Environment and Safety Engineering, North University of China, Taiyuan 030051, China

<sup>5</sup> State Key Laboratory of Fine Chemicals, School of Chemical Engineering, Dalian University of Technology, Dalian 116024, China

\* Correspondence: ccliu@nuc.edu.cn (C.L.); guoli@nuc.edu.cn (L.G.)

**Abstract:** Magnesium hydride (MgH<sub>2</sub>) has attracted considerable interest due to a number of favourable characteristics for hydrogen production via hydrolysis. In this study, MgH<sub>2</sub>-NaH composites with varying composition ratios were prepared by ball milling for different durations. The hydrogen production performances and enhancement mechanisms were subjected to meticulous investigation. The results revealed that the hydrogen production rate and kinetic properties of the composites were significantly improved with the rise in NaH content. For the MgH<sub>2</sub>-10 wt% NaH composites, the hydrogen production rate exhibited an initial increase followed by a subsequent decrease with the prolongation of ball milling. It is noteworthy that the hydrolysis of the composites in deionised water exhibited a significant improvement in reaction kinetics even after a mere 1 h of ball milling, releasing 1119 mL g<sup>-1</sup> of hydrogen in 30 s, with a conversion rate of 69.2%. The highest hydrolysis hydrogen generation rate of the 10 h milled MgH<sub>2</sub>-10 wt% NaH composite in deionised water at 30 °C was 1360 mL g<sup>-1</sup>, with a hydrogen conversion rate of 83.7% and a hydrolysis activation energy of 17.79 kJ mol<sup>-1</sup>. The notable improvement in the hydrolysis performance of the MgH<sub>2</sub>-NaH composite is attributed to the rapid generation of high temperatures at the interface, resulting from the exothermic reaction of sodium hydride hydrolysis.

**Keywords:** MgH<sub>2</sub>; NaH; ball milling; hydrolysis for hydrogen production; activation energy



**Citation:** Zhang, Z.; Li, Z.; Zhao, W.; Zhang, Y.; Peng, C.; Liu, C.; Guo, L. Ultrafast Hydrogen Production via Hydrolysis of MgH<sub>2</sub>-NaH Composite. *Metals* **2024**, *14*, 1038. <https://doi.org/10.3390/met14091038>

Academic Editor: Claudio Pistidda

Received: 6 August 2024

Revised: 3 September 2024

Accepted: 9 September 2024

Published: 12 September 2024



**Copyright:** © 2024 by the authors. Licensee MDPI, Basel, Switzerland. This article is an open access article distributed under the terms and conditions of the Creative Commons Attribution (CC BY) license (<https://creativecommons.org/licenses/by/4.0/>).

## 1. Introduction

Today, the world energy structure is still predominantly reliant on traditional fossil fuels: coal, oil, and natural gas. However, the traditional fossil energy reserves are limited and non-renewable. Their combustion emits significant quantities of pollutant gases, such as CO<sub>2</sub>, Sox, and NO<sub>x</sub>, leading to serious environmental issues like greenhouse effects, acid rain, and haze [1]. Consequently, the development of clean and sustainable renewable energy and new materials is critical for human sustainability [2]. Hydrogen energy is widely considered as the most promising alternative energy carrier to traditional fossil fuels due to its abundant availability, high energy density (142 MJ/kg), and clean and non-polluting nature [3–6]. Hydrogen fuel cells, which use hydrogen as their “fuel”, are one of the most attractive new energy sources, making efficient and safe hydrogen production technology particularly important [7–9].

In recent years, hydrogen production based on the hydrolysis of light metals and hydrides, such as MgH<sub>2</sub>, NaBH<sub>4</sub>, CaH<sub>2</sub>, and LiH, has garnered considerable attention. These systems offer significant potential for seamless integration into a wide range of applications.

The hydrolysis of hydrides presents an effective on-demand hydrogen production method that can be readily integrated into various mobile applications [10–12]. Many researchers are currently focusing on hydrogen production from the hydrolysis of metal hydrides and chemical hydrides, such as  $\text{MgH}_2$ ,  $\text{NaBH}_4$ ,  $\text{CaH}_2$ , and  $\text{LiH}$ . The theoretical hydrogen yields of the above materials are 15.32 wt%, 21.32 wt%, 9.58 wt%, and 25.36 wt%, respectively, without considering water consumption. Among them,  $\text{NaBH}_4$  has been considered as a promising material due to its high hydrogen storage density. However, its reliance on precious metal catalysts and the issue of by-product recovery result in high cost [13–15]. Additionally,  $\text{CaH}_2$  and  $\text{LiH}$  react violently with water, making the experimental process difficult to control [16,17].  $\text{NaMgH}_3$  was synthesised by grinding an equimolar mixture of  $\text{NaH}$  and  $\text{MgH}_2$  for 40 h and hydrogenating it in a reaction cell filled with 5 MPa hydrogen for 5 h at 623 K to obtain high-purity  $\text{NaMgH}_3$  [18]. The synthesised substance was further hydrolysed at room temperature to give an instantaneous hydrogen production of  $1360 \text{ mL g}^{-1}$ .

In contrast, the hydrolysis of  $\text{MgH}_2$  can be performed at room temperature and standard atmospheric pressure without the need of expensive catalysts [19–23]. Furthermore, the by-product of this reaction,  $\text{Mg(OH)}_2$ , can be used directly as a flame retardant and is environmentally friendly and non-polluting. Therefore,  $\text{MgH}_2$  is considered as one of the most promising materials for hydrogen production through hydrolysis [24–26].

However, the dense passivation layer of  $\text{Mg(OH)}_2$ , formed during hydrolysis, hinders further contact between water and the inner  $\text{MgH}_2$ , resulting in slow hydrolysis kinetics [27,28]. To address this issue and remove the passivation layer to promote the continuous hydrolysis reaction of  $\text{MgH}_2$ , researchers have explored various methods, including introducing different cations/anions into the solution [29,30], adding additives [31,32], incorporating organic and inorganic acids [20,33], and reducing the  $\text{MgH}_2$  particle size [34,35]. These approaches have improved the hydrolysis kinetics and hydrogen production rate of the hydrolysis reaction to some extent. However, some challenges remain with the above method, such as the corrosivity and low hydrogen capacity associated with the addition of acid or salt solutions, as well as the overall slow kinetics of the hydrolysis process.

Light metal hydrides are renowned for their high hydrogen storage capacities and catalytic activities, which have been shown to enhance the hydrolysis of  $\text{MgH}_2$ . However, research into the catalytic mechanisms and the impact of adding  $\text{NaH}$  to the  $\text{MgH}_2$  system remains limited. This paper introduces  $\text{NaH}$  as an effective catalytic agent to improve  $\text{MgH}_2$ 's hydrolysis performance.  $\text{NaH}$ , as a potent catalyst, can integrate high hydrogen conversion rates with rapid hydrolysis reaction rates, thus further enhancing the hydrolysis efficiency of  $\text{MgH}_2$ . In this study,  $\text{NaH}$  was incorporated as a promoter, and a series of  $\text{MgH}_2$ - $X$  wt%  $\text{NaH}$  ( $X = 5, 10, 30, \text{ and } 50$ ) composite materials were synthesised using high-energy ball milling to optimise the hydrolysis performance of  $\text{MgH}_2$ . We systematically examined the effects of ball milling duration, reaction temperature, and  $\text{NaH}$  concentration on the kinetics and hydrogen production rate of  $\text{MgH}_2$  hydrolysis. The chemical composition and microstructure of the  $\text{MgH}_2$ -based composite materials and hydrolysis products were characterised using X-ray diffraction (XRD), scanning electron microscopy (SEM), and other analytical techniques. Additionally, real-time temperature and pH measurements were employed to elucidate the catalytic hydrolysis mechanism of  $\text{NaH}$  on  $\text{MgH}_2$ . The findings aim to advance the development of high-performance  $\text{MgH}_2$  systems to achieve superior hydrolysis performance. Light metal hydrides, known for their high hydrogen storage capacities and catalytic activities, have been shown to benefit the hydrolysis of  $\text{MgH}_2$ .

## 2. Experiments

### 2.1. Preparation of $\text{MgH}_2$ - $\text{NaH}$ Composites

The additive composites of  $\text{MgH}_2$ - $x$  wt%  $\text{NaH}$  ( $x = 5, 10, 30, 50$ ) were prepared using a planetary milling machine (QM-3SP4) with steel balls and mechanically ball-milled for durations of 1, 5, 10, and 15 h. The ball-to-powder ratio was maintained at 30:1, and the rotational speed was set at 521 rpm under an argon atmosphere to prevent oxidation.

The specific procedure alternated between 30 min of ball milling and 10 min of cooling to mitigate the heat effects during ball milling. In order to avoid the exposure of the composites to oxygen and water, all the samples were processed in a glove box under an argon atmosphere, with oxygen and water concentrations  $<0.01$  ppm.

## 2.2. Structural Characterisation of Materials

The phase compositions of the samples and hydrolysis products were analysed by X-ray diffraction (XRD, Panalytical Empyrean, Almelo, The Netherlands) using Cu radiation. The XRD analysis was carried out over a range of  $5^\circ$  to  $90^\circ$  with a scanning speed of  $5^\circ \text{ min}^{-1}$ . Field emission scanning electron microscopy (SEM) was used to observe the elemental distribution and surface morphology of the  $\text{MgH}_2$  matrix composites as well as the hydrolysis products.

Due to the high reactivity of the prepared hydrogen production composite powder, a customised sample holder was developed to prevent the oxidation of the samples during the structural analysis of  $\text{MgH}_2$ -based composite hydrogen production materials using X-ray diffraction (XRD). This holder was sealed with XRD transparent film, and samples were loaded in an argon atmosphere glove box. This process ensures that the composite materials are not oxidised, thus guaranteeing the accuracy of the test results.

## 2.3. Hydrogen Hydrolysis Performance Test

The hydrolysis setup used in this work is shown in Figure 1. The hydrolysis properties of  $\text{MgH}_2$ -based composites in deionised water were determined using the drained gas collection method. An electronic balance (model: HZY-B2200, Huazhi Electronic Technology Co., Ltd., Putian, China) was used to measure the mass of water replaced by the released hydrogen, and the number shown on the balance could be directly converted to the volume of hydrogen produced by hydrolysis. The electronic balance was connected to a computer, which can automatically record the real-time hydrogen yield as well as the temperature, pH data, and reaction time throughout the process. Temperature and pH measurements were collected by an acidometer (model: Sartorius Pb-30L) connected to one end of a three-necked flask. In this experiment, the hydrogen yield of the sample was calculated by hydrolysing 0.1 g of the composite sample and then converting it to the hydrogen yield under the standard condition using the ideal gas equation. The hydrogen conversion rate was calculated by dividing the actual hydrogen production volume by the theoretical hydrogen production volume of the composites. The hydrogen generation rate (mHGR) refers to the instantaneous hydrogen release rate, the maximum value of which is derived from the differential curve of the hydrogen production over time. To investigate the activation energy of the studied samples, the reaction temperature was adjusted to allow for the hydrolysis of  $\text{MgH}_2$ -based composites milled for different durations (1, 5, 10, and 15 h) at various temperatures (30, 40, 50, and  $60^\circ\text{C}$ ). Each experiment was repeated three times to ensure accuracy. Hydrolysis products were obtained by filtering the hydrolysed solution and drying it in a blast oven at  $60^\circ\text{C}$  overnight.

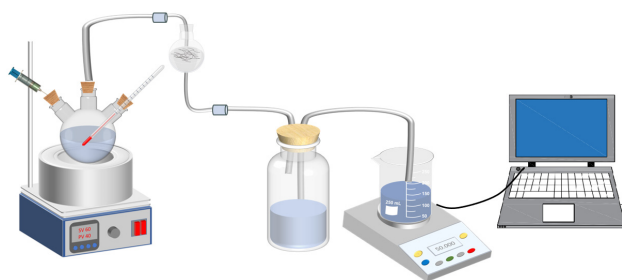


**Figure 1.** A schematic diagram of the hydrolysis unit.

### 3. Experimental Results and Discussion

#### 3.1. Effect of NaH Addition Content

Figures 1–3 show the XRD patterns of  $\text{MgH}_2$  ball-milled with different contents of NaH for 10 h. The XRD results indicate that the product is composed of  $\text{MgH}_2$  and NaH. Additionally, the XRD patterns reveal the presence of  $\text{NaMgH}_3$ , a new substance with a perovskite structure. This suggests that NaH could react with  $\text{MgH}_2$  to form  $\text{NaMgH}_3$  during ball milling, which is consistent with the findings of Wang et al. [18]. In addition, it can also be seen from Figure 2 that the diffraction peaks of  $\text{NaMgH}_3$  increase significantly with the higher NaH addition content. When the mass percentages of  $\text{MgH}_2$  and NaH are equal, the product is predominantly  $\text{NaMgH}_3$ .

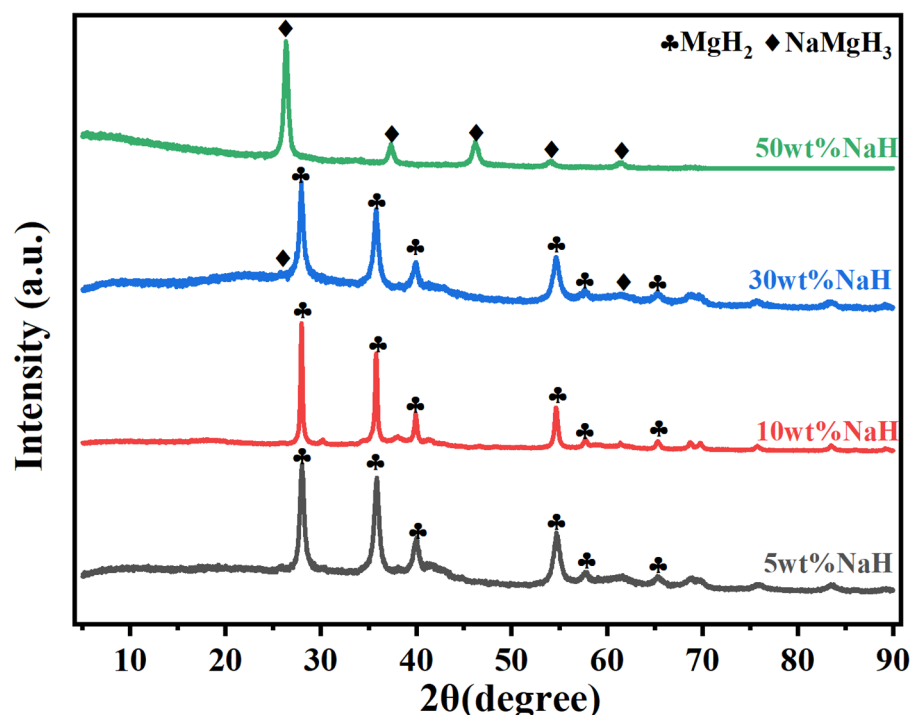


Figure 2. XRD patterns of  $\text{MgH}_2$ - $x$  wt% NaH ( $x = 5, 10, 30,$  and  $50$ ) composites ball-milled for 10 h.

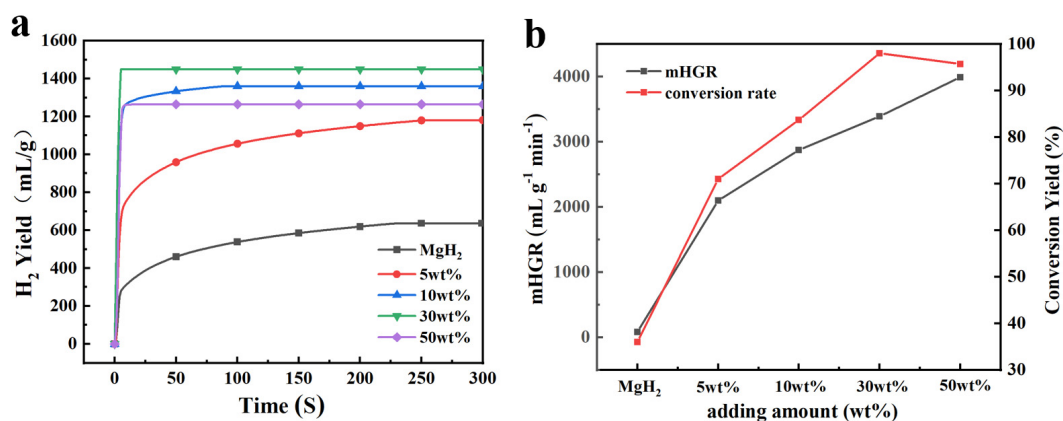
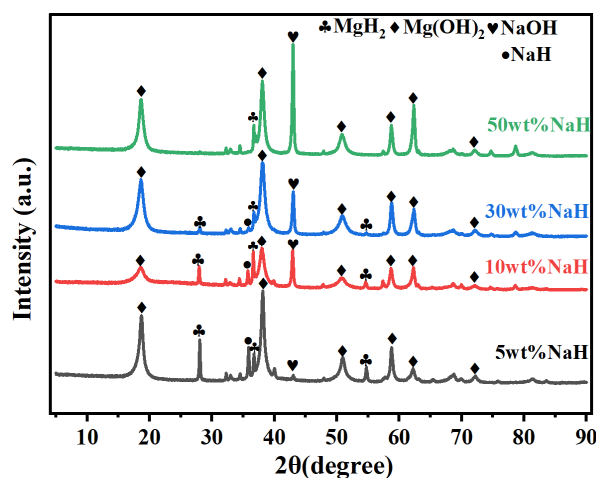


Figure 3. (a) Hydrogen generation curves, (b) conversion yield and mHGR of  $\text{MgH}_2$ - $x$  wt% NaH ( $x = 0, 5, 10, 30,$  and  $50$ ) composites milled for 10 h in deionised water at  $30^\circ\text{C}$ .

Figure 3a shows the hydrolysis curve of the  $\text{MgH}_2$ - $x$  wt% NaH composite in deionised water after 10 h of ball milling. The hydrolysis kinetics of 10 h ball-milled pure  $\text{MgH}_2$  in deionised water were very poor, producing only  $630 \text{ mL g}^{-1}$  of hydrogen in 10 min. It can be clearly seen that the hydrolysis performance was significantly improved by adding a

small amount of NaH. The MgH<sub>2</sub>-5 wt% NaH composite could produce 1181 mL g<sup>-1</sup> of hydrogen with a conversion rate of 73.1%, which is about twice that of pure MgH<sub>2</sub> [30]. As NaH content increased, the rate of hydrogen production also increased, but the amount of hydrogen produced first rose and then fell. This decline is due to the fact that the hydrogen storage capacity of the composite decreases with higher NaH content, and therefore, the amount of hydrogen production decreases. Figure 3b illustrate that the maximum instantaneous hydrogen production rate (mHGR) increased from 2098 mL g<sup>-1</sup> min<sup>-1</sup> to 3989 mL g<sup>-1</sup> min<sup>-1</sup> as the NaH content increased from 5 wt% to 50 wt%. Concurrently, the hydrolysis hydrogen production rose from 1181 mL g<sup>-1</sup> to 1448.5 mL g<sup>-1</sup> and then slightly decreased to 1264 mL g<sup>-1</sup>. Although a high NaH content can greatly increase the reaction rate at the initial stage of hydrolysis, it reduces the overall continuity of the hydrolysis reaction and the hydrogen storage capacity of the composites, leading to a decrease in the total amount of hydrogen produced by hydrolysis. Additionally, an excessively high NaH mass ratio can make the reaction too violent, compromising the safety of the experiment. Therefore, 10 wt% NaH should be considered as the optimal addition amount [23].

To further investigate the hydrolysis process of the composite materials, X-ray diffraction (XRD) was conducted on the by-products of MgH<sub>2</sub> with varying NaH content (5, 10, 30, and 50 wt%). As shown in Figure 4, the primary hydrolysis products are Mg(OH)<sub>2</sub>, NaOH, and residual, unreacted MgH<sub>2</sub> and NaH. The diffraction peaks corresponding to MgH<sub>2</sub> diminish as the NaH content increases. This reduction in residual MgH<sub>2</sub> indicates a higher hydrolysis conversion rate, consistent with the results presented in Figure 3a.



**Figure 4.** XRD plots of hydrolysis products of MgH<sub>2</sub>-x wt% NaH (x = 5, 10, 30, and 50) composites in deionised water at 30 °C.

The above experimental results demonstrated that the addition of NaH is beneficial to the improvement in the hydrolysis hydrogen production performance of MgH<sub>2</sub>. In order to further explore the effects of the catalytic mechanism of NaH in enhancing the hydrolysis hydrogen production performance of MgH<sub>2</sub>, the real-time temperature and pH throughout the reaction stage of 10 h ball-milled MgH<sub>2</sub>-x wt% NaH composites in deionised water were analysed. As shown in Figure 5a,b, the instantaneous temperature rose to 4, 7, 10, and 11.8 °C within 10 s for NaH addition contents of 5, 10, 30, and 50 wt%, respectively. The temperature gradually decreased and tended to be constant as the reaction progressed [33]. With the increase in NaH content, both the instantaneous temperature and the pH of the reaction solution increased sharply. For the sample with the addition of 50 wt% of NaH, the instantaneous temperature rose to 11.8 °C in 10 s. This rapid temperature rise is attributed to the exothermic reaction of NaH hydrolysis [10]. The instantaneous

high reaction temperature in the interface further increases the reaction rate of  $\text{MgH}_2$  hydrolysis, which is consistent with the results shown in Figure 3a.

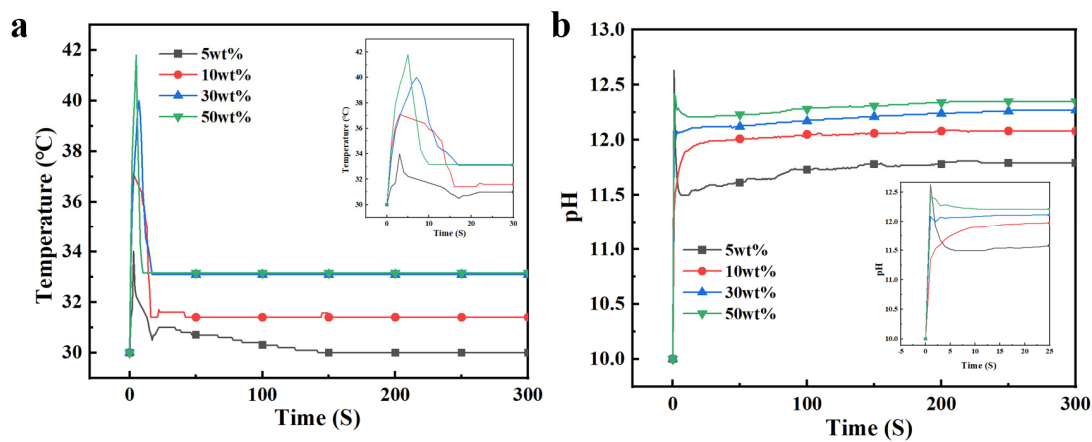


**Figure 5.** (a) Real-time temperature profiles and (b) pH profiles of  $\text{MgH}_2-x$  wt.% NaH ( $x = 5, 10, 30,$  and  $50$ ) composites milled for 10 h in deionised water at  $30^\circ\text{C}$ .

### 3.2. Effect of Temperature on Hydrolysis Properties of $\text{MgH}_2\text{-NaH}$ Composites

The reaction temperature also plays an important role in the hydrolysis of  $\text{MgH}_2$ . In order to investigate the effect of temperature on the hydrolysis performance of the composites, the  $\text{MgH}_2\text{-10 wt\% NaH}$  composite ball-milled for 10 h was tested in deionised water at  $30, 40, 50,$  and  $60^\circ\text{C}$ . The hydrolysis curves are shown in Figure 5a. It is indicated that the hydrolysis reaction rate and the hydrogen yields gradually increased with the rising solution temperature. When the temperature increased from  $30$  to  $60^\circ\text{C}$ , the hydrolysis hydrogen production of  $\text{MgH}_2\text{-10 wt\% NaH}$  composites increased from  $1360.1\text{ mL g}^{-1}$  to  $1422.7$  ( $40^\circ\text{C}$ ),  $1536.2$  ( $50^\circ\text{C}$ ), and  $1601.6$  ( $60^\circ\text{C}$ )  $\text{mL g}^{-1}$ .

The fitting of the hydrolysis curves at different temperatures reveals a good linear relationship between both  $\ln(k)$  and  $1/T$  for the hydrolysis reaction of the  $\text{MgH}_2\text{-10 wt\% NaH}$  composite, according to the Arrhenius equation:

$$\ln k = \ln A - Ea/RT$$

where  $k$  is the reaction rate constant,  $Ea$  is the activation energy,  $R$  is the gas constant  $8.314$  ( $8.314\text{ J mol}^{-1}\cdot\text{K}^{-1}$ ), and  $T$  is the temperature of the reaction (in Kelvin). The activation energy  $Ea$  for the hydrolysis of  $\text{MgH}_2$  catalysed by NaH can be calculated by multiplying the slope of the fitted straight line in Figure 6b by the gas fraction  $R$ . The calculation results show that the activation energy  $Ea$  for the hydrolysis of  $\text{MgH}_2$  is  $17.79\text{ kJ mol}^{-1}$  with the addition of NaH, which is substantially lower than that of pure  $\text{MgH}_2$  ( $58.058\text{ kJ mol}^{-1}$ ) [26]. This reduction in activation energy indicates that the hydrolysis reaction of  $\text{MgH}_2$  is more likely to occur after the addition of NaH. Compared to the other additives reported in Table 1, the  $\text{MgH}_2$  composite with NaH in this study demonstrates a lower hydrolysis activation energy, suggesting that the  $\text{MgH}_2\text{-10 wt\% NaH}$  composite exhibits superior hydrolysis performance.

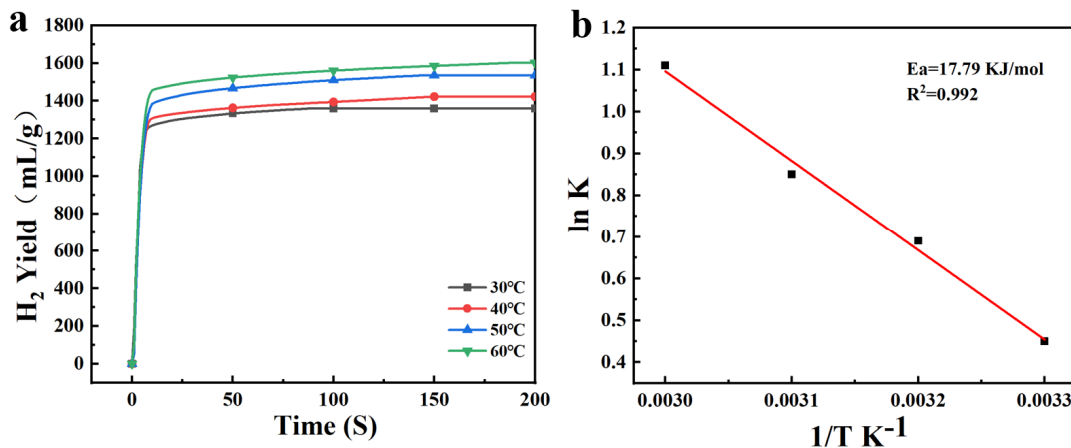


**Figure 6.** (a) Hydrogen generation curves of MgH<sub>2</sub>–10 wt% NaH composite milled for 10 h in deionised water at different temperatures, (b) Arrhenius plot of hydrolysis of MgH<sub>2</sub>–10 wt% NaH composite.

**Table 1.** A comparison of the activation energy of the hydrogen generation reaction for various MgH<sub>2</sub> composite systems.

Materials	Hydrolysis Solution	$E_a$ (kJ mol <sup>-1</sup> )	Ref.
MgH <sub>2</sub> –10 wt% NaH	deionised water	17.79	This work
MgH <sub>2</sub> –10 wt% CoCl <sub>2</sub>	deionised water	31.3	[27]
MgH <sub>2</sub> (HCS)	0.1 M AlCl <sub>3</sub> solution	34.68	[21]
MgH <sub>2</sub> (HCS)	0.5 M AlCl <sub>3</sub> solution	21.64	[21]
16MgH <sub>2</sub> –LiNH <sub>2</sub>	pure water	37.40	[10]
MgH <sub>2</sub>	0.5 M Fe <sub>2</sub> (SO <sub>4</sub> ) <sub>3</sub> solution	19.15	[23]

### 3.3. Effect of Ball Milling Time on Hydrogen Production Performance of MgH<sub>2</sub>-10 wt% NaH

In addition to NaH content and hydrolysis temperature, ball milling time is also a crucial factor affecting the hydrolysis performance of MgH<sub>2</sub> for hydrogen production. MgH<sub>2</sub> mixed with 10 wt% NaH was ball-milled for different times (1, 5, 10, and 15 h) and subsequently tested for its hydrolysis performance in deionised water. Figure 7a shows the hydrolysis hydrogen production curves of MgH<sub>2</sub>-10 wt% NaH ball-milled for different durations. The figure indicates that all the composites exhibit excellent hydrolysis hydrogen production performance compared to pure magnesium hydride, underscoring the significant enhancement effect of NaH addition during ball milling. It is notable that, even after just 1 h of ball milling, the hydrolysis of composites in deionised water showed a remarkable improvement in kinetics, releasing 1119 mL g<sup>-1</sup> of hydrogen in 30 s, with a conversion rate of 69.2%, which could be considered as a nearly instantaneous completion of hydrogen production. As shown in Figure 7a,b, the hydrolysis hydrogen production and maximum hydrogen generation rate (mHGR) of the MgH<sub>2</sub>-10 wt% NaH composites initially increased with longer ball milling time, reaching a peak before declining. Specifically, the highest hydrolysis hydrogen production and mHGR were achieved after 10 h of ball milling, with values of 1360 mL g<sup>-1</sup> and 2873.5 mL g<sup>-1</sup> min<sup>-1</sup>, respectively. However, extending the ball milling time to 15 h resulted in a decrease in hydrogen production and mHGR to 1262 mL g<sup>-1</sup> and 2707 mL g<sup>-1</sup> min<sup>-1</sup>, respectively.

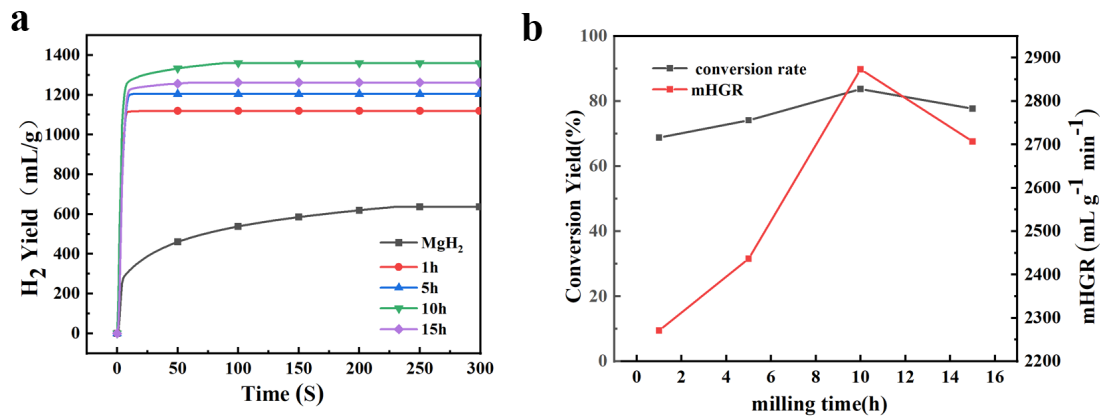


**Figure 7.** (a) Hydrogen generation curves, (b) conversion yield and mHGR of MgH<sub>2</sub>–10 wt% NaH composite milled for different times in deionised water at 30 °C.

Ball milling is widely recognised as a highly effective and straightforward technique for altering particle size and morphology, which can significantly influence the hydrolysis properties of magnesium-based materials. It can be seen that the ball milling time has a great influence on the hydrolysis performance of the MgH<sub>2</sub>-NaH system. With the prolongation of the ball milling time, the reaction rate increases, and the hydrolysis hydrogen production and mHGR first increase and then decrease. The observed decrease in hydrolysis hydrogen production and mHGR with the prolongation of ball milling time, as shown in Figure 7a, could be attributed to the prolonged ball milling time disrupting the structure of NaMgH<sub>3</sub>. This disruption leads to the loss of a significant number of active sites and the agglomeration of MgH<sub>2</sub> particles, which ultimately deteriorates the hydrolysis performance of MgH<sub>2</sub>. In order to further investigate the presence of the agglomeration, SEM analyses were performed on the micro-morphology of the MgH<sub>2</sub>-10 wt% NaH composites after different ball milling times. The results are presented in Figure 8a–d. Figure 8a–c reveal that as the ball milling time increased from 1 h to 10 h, MgH<sub>2</sub> and NaH were broken up from the original lumps into smaller-sized particles. Additionally, NaH became more uniformly dispersed within the matrix of MgH<sub>2</sub> (Figure 8c). This improvement in dispersion is mainly due to NaH acting as an effective grinding aid during the ball milling process, preventing MgH<sub>2</sub> particles from agglomerating and thereby refining their size. However, when the ball milling time was extended to 15 h, it can be seen from Figure 8d that the structure of NaH was severely damaged, causing it to lose its grinding aid effect. As a result, MgH<sub>2</sub> began to agglomerate into large particles, negatively impacting its hydrolysis performance.

To evaluate the dispersion of the NaH additive within the composite materials, Energy-Dispersive Spectroscopy (EDS) was performed on the MgH<sub>2</sub>-10 wt% NaH composite after 10 h of ball milling. The results, depicted in Figure 9a–c, reveal that extensive ball milling results in a uniform distribution of NaH throughout the composite. The NaH particles are finely and evenly dispersed across the surface of the MgH<sub>2</sub>. This uniform dispersion significantly enhances the hydrolysis activity of the composite, leading to a marked improvement in its hydrolysis kinetics.

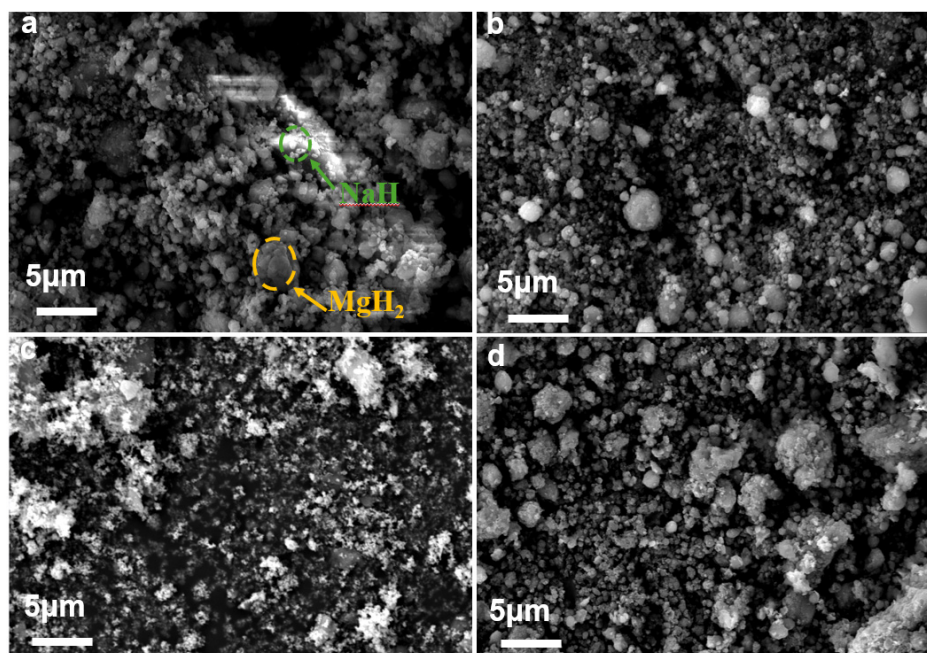


**Figure 8.** SEM images of  $\text{MgH}_2$ –10 wt% NaH composites ball-milled for different times: (a) 1 h; (b) 5 h; (c) 10 h; (d) 15 h.

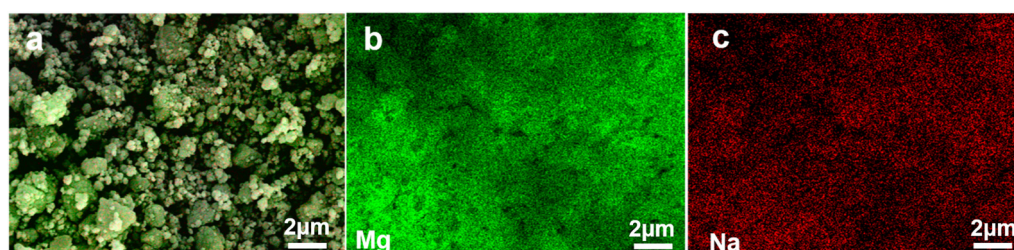


**Figure 9.** SEM images of  $\text{MgH}_2$ –10 wt% NaH composites (a) and corresponding elemental distribution map of magnesium (b), and Sodium (c).

#### 4. Conclusions

In this paper, highly active  $\text{MgH}_2$ -NaH composites were prepared and synthesised via planetary ball milling, with NaH serving as the catalyst for  $\text{MgH}_2$ . The impacts of NaH content, ball milling duration, and hydrolysis temperature on the hydrolysis properties of these composites were carefully investigated.

1.  $\text{MgH}_2$ -NaH composites prepared by mechanical ball milling have excellent hydrolysis properties. The hydrolysis reaction kinetics of  $\text{MgH}_2$  can be significantly improved by adding a trace amount of NaH. The hydrogen production of  $\text{MgH}_2$ -5 wt% NaH composites was  $830 \text{ mL g}^{-1}$  hydrogen in 20 s, which is 50% of the theoretical hydrogen production, and this can be regarded as almost instantaneous hydrogen production. With the increase in NaH addition content, this instantaneous hydrogen production effect was continuously amplified while ensuring high hydrogen production, which further enhanced the hydrolysis reaction rate and shortened the reaction time.
2. The increase in temperature can improve the hydrolysis hydrogen production performance of composites. By analysing hydrolysis curves at different temperatures, the activation energy of the hydrolysis reaction of  $\text{MgH}_2$ -10 wt% NaH was determined to be  $17.79 \text{ kJ mol}^{-1}$ , indicating a significant reduction compared to pure  $\text{MgH}_2$ . The highest hydrolysis hydrogen production and mHGR were achieved after 10 h of ball milling, with values of  $1360 \text{ mL g}^{-1}$  and  $2873.5 \text{ mL g}^{-1} \text{ min}^{-1}$ , respectively.

**Author Contributions:** Conceptualisation, Z.Z. and L.G.; methodology, Z.Z. and Z.L.; validation, W.Z. and Y.Z.; formal analysis, W.Z.; investigation, Z.Z. and Z.L.; data curation, W.Z. and Y.Z.; writing—original draft preparation, Z.Z. and Z.L.; writing—review and editing, C.P. and C.L.; visualisation, Z.L.; supervision, C.L.; project administration, L.G.; funding acquisition, Z.Z. and C.P. All authors have read and agreed to the published version of the manuscript.

**Funding:** The APC was funded by [the National Natural Science Foundation of China (52301292), the Fundamental Research Program of Shanxi Province (202103021223193), Shanxi Scholarship Council of China (2023-144), and Fundamental Research Funds for the Central Universities (DUT23RC(3)044)].

**Data Availability Statement:** The original contributions presented in the study are included in the article, further inquiries can be directed to the corresponding authors.

**Conflicts of Interest:** Authors Zhao Zhang, Zhenji Li, Wei Zhao, Changcheng Liu and Li Guo were employed by the company Shanxi Key Laboratory of Efficient Hydrogen Storage & Production Technology and Application. Author Zhao Zhang was employed by the company State Key Laboratory of Coal and CBM Co-Mining. The remaining authors declare that the research was conducted in the absence of any commercial or financial relationships that could be construed as a potential conflict of interest.

## References

1. Liu, J.; Zhang, B.; Yu, H.; Li, T.; Hu, M.; Yang, J. A novel oxidation-resistible Mg@Ni foam material for safe, efficient, and controllable hydrogen generation. *J. Magnes. Alloys* **2023**, *in press*. [[CrossRef](#)]
2. Rusman, N.A.A.; Dahari, M. A review on the current progress of metal hydrides material for solid-state hydrogen storage applications. *Int. J. Hydrogen Energy* **2016**, *41*, 12108–12126. [[CrossRef](#)]
3. Sakintuna, B.; Lamaridarkrim, F.; Hirscher, M. Metal hydride materials for solid hydrogen storage: A review☆. *Int. J. Hydrogen Energy* **2007**, *32*, 1121–1140. [[CrossRef](#)]
4. Muir, S.S.; Yao, X. Progress in sodium borohydride as a hydrogen storage material: Development of hydrolysis catalysts and reaction systems. *Int. J. Hydrogen Energy* **2011**, *36*, 5983–5997. [[CrossRef](#)]
5. Xingguo, L.L.; Jie, Z.; Xiaojuan, W.U.; Shunpeng, C.; Jifeng, D. Recent Progress on Materials for Hydrogen Generation via Hydrolysis. *J. Inorg. Mater.* **2021**, *36*, 1–8. [[CrossRef](#)]
6. Olabi, A.G.; Abdelghafar, A.A.; Baroutaji, A.; Sayed, E.T.; Alami, A.H.; Rezk, H.; Abdelkareem, M.A. Large-scale hydrogen production and storage technologies: Current status and future directions. *Int. J. Hydrogen Energy* **2021**, *46*, 23498–23528. [[CrossRef](#)]
7. Li, Y.; Lee, L.Q.; Zhao, H.; Zhao, Y.; Gao, P.; Li, H. Alcohol–alkali hydrolysis for high-throughput PET waste electroreforming-assisted green hydrogen generation. *J. Mater. Chem. A* **2024**, *12*, 2121–2128. [[CrossRef](#)]
8. Urbonavicius, M.; Varnagiris, S.; Knoks, A.; Mezulis, A.; Kleperis, J.; Richter, C.; Meirbekova, R.; Gunnarsson, G.; Milcius, D. Enhanced Hydrogen Generation through Low-Temperature Plasma Treatment of Waste Aluminum for Hydrolysis Reaction. *Materials* **2024**, *17*, 2637. [[CrossRef](#)] [[PubMed](#)]
9. Hammad, A.; Ning, F.; Zou, S.; Liu, Y.; Tian, B.; He, C.; Chai, Z.; Wen, Q.; He, L.; Zhou, X. Aluminum hydrolysis for hydrogen generation enhanced by sodium hydride. *Int. J. Hydrogen Energy* **2024**, *77*, 138–148. [[CrossRef](#)]
10. Ma, M.; Ouyang, L.; Liu, J.; Wang, H.; Shao, H.; Zhu, M. Air-stable hydrogen generation materials and enhanced hydrolysis performance of MgH<sub>2</sub>-LiNH<sub>2</sub> composites. *J. Power Sources* **2017**, *359*, 427–434. [[CrossRef](#)]
11. Wei, Y.; Wang, M.; Fu, W.; Wei, L.; Zhao, X.; Zhou, X.; Ni, M.; Wang, H. Highly active and durable catalyst for hydrogen generation by the NaBH<sub>4</sub> hydrolysis reaction: CoWB/NF nanodendrite with an acicular array structure. *J. Alloys Compd.* **2020**, *836*, 155429. [[CrossRef](#)]
12. Huang, C.; Yu, Y.; Tang, X.; Liu, Z.; Zhang, J.; Ye, C.; Ye, Y.; Zhang, R. Hydrogen generation by ammonia decomposition over Co/CeO<sub>2</sub> catalyst: Influence of support morphologies. *Appl. Surf. Sci.* **2020**, *532*, 147335. [[CrossRef](#)]
13. Lei, W.; Jin, H.; Gao, J.; Chen, Y. Efficient hydrogen generation from the NaBH<sub>4</sub> hydrolysis by amorphous Co–Mo–B alloy supported on reduced graphene oxide. *J. Mater. Res.* **2021**, *36*, 4154–4168. [[CrossRef](#)]
14. Li, Z.; Xu, Y.; Guo, Q.; Li, Y.; Ma, X.; Li, B.; Zhu, H.; Yuan, C.-G. Preparation of Ag@PNCMs nanocomposite as an effective catalyst for hydrogen generation from hydrolysis of sodium borohydride. *Mater. Lett.* **2021**, *297*, 129828. [[CrossRef](#)]
15. Deng, J.; Sun, B.; Xu, J.; Shi, Y.; Xie, L.; Zheng, J.; Li, X. A monolithic sponge catalyst for hydrogen generation from sodium borohydride solution for portable fuel cells. *Inorg. Chem. Front.* **2021**, *8*, 35–40. [[CrossRef](#)]
16. Balbay, A.; Saka, C. Semi-methanolysis reaction of potassium borohydride with phosphoric acid for effective hydrogen production. *Int. J. Hydrogen Energy* **2018**, *43*, 21299–21306. [[CrossRef](#)]
17. Qiu, H.; Han, X.; Zang, S.; Liu, W.; Yang, G.; Lv, L.; Wang, X.; Duan, J.; Wang, S. Effect of LiH on the fast hydrolysis and hydrogen generation of MgH<sub>2</sub> by ball milling. *New J. Chem.* **2022**, *46*, 19900–19908. [[CrossRef](#)]
18. Wang, H.; Zhang, J.; Liu, J.W.; Ouyang, L.Z.; Zhu, M. Catalysis and hydrolysis properties of perovskite hydride NaMgH<sub>3</sub>. *J. Alloys Compd.* **2013**, *580*, S197–S201. [[CrossRef](#)]

19. Kushch, S.D.; Kuyunko, N.S.; Nazarov, R.S.; Tarasov, B.P. Hydrogen-generating compositions based on magnesium. *Int. J. Hydrogen Energy* **2011**, *36*, 1321–1325. [[CrossRef](#)]
20. Tayeh, T.; Awad, A.S.; Nakhl, M.; Zakhour, M.; Silvain, J.F.; Bobet, J.L. Production of hydrogen from magnesium hydrides hydrolysis. *Int. J. Hydrogen Energy* **2014**, *39*, 3109–3117. [[CrossRef](#)]
21. Verbovytsky, Y.V.; Berezovets, V.V.; Kytsya, A.R.; Zavaliy, I.Y.; Yartys, V.A. Hydrogen Generation by the Hydrolysis of MgH<sub>2</sub>. *Mater. Sci.* **2020**, *56*, 1–14. [[CrossRef](#)]
22. Kojima, Y. Hydrogen generation by hydrolysis reaction of lithium borohydride. *Int. J. Hydrogen Energy* **2004**, *29*, 1213–1217. [[CrossRef](#)]
23. Yuan, C.; Chen, W.; Yang, Z.; Huang, Z.; Yu, X. The effect of various cations/anions for MgH<sub>2</sub> hydrolysis reaction. *J. Mater. Sci. Technol.* **2021**, *73*, 186–192. [[CrossRef](#)]
24. Chen, J.; Fu, H.; Xiong, Y.; Xu, J.; Zheng, J.; Li, X. MgCl<sub>2</sub> promoted hydrolysis of MgH<sub>2</sub> nanoparticles for highly efficient H<sub>2</sub> generation. *Nano Energy* **2014**, *10*, 337–343. [[CrossRef](#)]
25. Gao, H.; Shi, R.; Zhu, J.; Liu, Y.; Shao, Y.; Zhu, Y.; Zhang, J.; Li, L.; Hu, X. Interface effect in sandwich like Ni/Ti<sub>3</sub>C<sub>2</sub> catalysts on hydrogen storage performance of MgH<sub>2</sub>. *Appl. Surf. Sci.* **2021**, *564*, 150302. [[CrossRef](#)]
26. Huang, M.; Ouyang, L.; Wang, H.; Liu, J.; Zhu, M. Hydrogen generation by hydrolysis of MgH<sub>2</sub> and enhanced kinetics performance of ammonium chloride introducing. *Int. J. Hydrogen Energy* **2015**, *40*, 6145–6150. [[CrossRef](#)]
27. Zhou, C.; Zhang, J.; Zhu, Y.; Liu, Y.; Li, L. Controllable hydrogen generation behavior by hydrolysis of MgH<sub>2</sub>-based materials. *J. Power Sources* **2021**, *494*, 229726. [[CrossRef](#)]
28. Liu, P.; Wu, H.; Wu, C.; Chen, Y.; Xu, Y.; Wang, X.; Zhang, Y. Microstructure characteristics and hydrolysis mechanism of Mg–Ca alloy hydrides for hydrogen generation. *Int. J. Hydrogen Energy* **2015**, *40*, 3806–3812. [[CrossRef](#)]
29. Al Bacha, S.; Thienpont, A.; Zakhour, M.; Nakhl, M.; Bobet, J.L. Clean hydrogen production by the hydrolysis of magnesium-based material: Effect of the hydrolysis solution. *J. Clean. Prod.* **2021**, *282*, 124498. [[CrossRef](#)]
30. Su, M.; Hu, H.; Gan, J.; Ye, W.; Zhang, W.; Wang, H. Thermodynamics, kinetics and reaction mechanism of hydrogen production from a novel Al alloy/NaCl/g-C<sub>3</sub>N<sub>4</sub> composite by low temperature hydrolysis. *Energy* **2021**, *218*, 119489. [[CrossRef](#)]
31. Pighin, S.A.; Urretavizcaya, G.; Bobet, J.L.; Castro, F.J. Nanostructured Mg for hydrogen production by hydrolysis obtained by MgH<sub>2</sub> milling and dehydriding. *J. Alloys Compd.* **2020**, *827*, 154000. [[CrossRef](#)]
32. Oh, S.; Cho, T.; Kim, M.; Lim, J.; Eom, K.; Kim, D.; Cho, E.; Kwon, H. Fabrication of Mg–Ni–Sn alloys for fast hydrogen generation in seawater. *Int. J. Hydrogen Energy* **2017**, *42*, 7761–7769. [[CrossRef](#)]
33. Hiraki, T.; Hiroi, S.; Akashi, T.; Okinaka, N.; Akiyama, T. Chemical equilibrium analysis for hydrolysis of magnesium hydride to generate hydrogen. *Int. J. Hydrogen Energy* **2012**, *37*, 12114–12119. [[CrossRef](#)]
34. Grosjean, M.; Zidoune, M.; Roue, L.; Huot, J. Hydrogen production via hydrolysis reaction from ball-milled Mg-based materials. *Int. J. Hydrogen Energy* **2006**, *31*, 109–119. [[CrossRef](#)]
35. Awad, A.S.; El-Asmar, E.; Tayeh, T.; Mauvy, F.; Nakhl, M.; Zakhour, M.; Bobet, J.L. Effect of carbons (G and CFs), TM (Ni, Fe and Al) and oxides (Nb<sub>2</sub>O<sub>5</sub> and V<sub>2</sub>O<sub>5</sub>) on hydrogen generation from ball milled Mg-based hydrolysis reaction for fuel cell. *Energy* **2016**, *95*, 175–186. [[CrossRef](#)]

**Disclaimer/Publisher’s Note:** The statements, opinions and data contained in all publications are solely those of the individual author(s) and contributor(s) and not of MDPI and/or the editor(s). MDPI and/or the editor(s) disclaim responsibility for any injury to people or property resulting from any ideas, methods, instructions or products referred to in the content.